HAL
open science

A Sufficient Condition for the Absence of Two-Dimensional Instabilities of an Elastic Plate in a Duct with Compressible Flow

Jean-François Mercier

To cite this version:

Jean-François Mercier. A Sufficient Condition for the Absence of Two-Dimensional Instabilities of an Elastic Plate in a Duct with Compressible Flow. SIAM Journal on Applied Mathematics, 2018, 78 (6), pp.3119-3144. 10.1137/18M1165761 . hal-02381057

HAL Id: hal-02381057

https://inria.hal.science/hal-02381057v1

Submitted on 26 Nov 2019

HAL is a multi-disciplinary open access archive for the deposit and dissemination of scientific research documents, whether they are published or not. The documents may come from teaching and research institutions in France or abroad, or from public or private research centers.

L'archive ouverte pluridisciplinaire **HAL**, est destinée au dépôt et à la diffusion de documents scientifiques de niveau recherche, publiés ou non, émanant des établissements d'enseignement et de recherche français ou étrangers, des laboratoires publics ou privés.

A SUFFICIENT CONDITION FOR THE ABSENCE OF 2D INSTABILITIES OF AN ELASTIC PLATE IN A DUCT WITH COMPRESSIBLE FLOW*

J-F. MERCIER†

Abstract. We study the time-harmonic resonance of a finite-length elastic plate in a fluid in uniform flow confined in a duct. Although the resonance frequencies are usually real, the combined effects of plate elasticity and of a flow can create complex frequencies, different from the usual so-called scattering frequencies, corresponding to instabilities. We study theoretically the existence of instabilities versus several problem parameters, notably the flow velocity and the ratio of densities and of sound speeds between the plate and the fluid. A 3D-volume in the parameters space is defined, in which no instability can develop. In particular it corresponds to a low enough velocity or a light enough plate. The theoretical estimates are validated numerically.

1. Introduction. We are interested in an acoustic fluid-structure problem: an elastic finite plate surrounded by a compressible uniform flow confined in a rigid waveguide. We consider the time harmonic regime: all the quantities vary like $e^{-i\omega t}$ where ω is the frequency.

In this paper we focus on the resonance frequencies: the frequencies for which there is non-uniqueness in the associated scattering problem, with a solution of the homogeneous problem in the L^2-space. It means that without any acoustic source, fluid vibrations and plate deformations, periodic in time and with finite energy, can exist. This solution is called a trapped mode since it is confined to the vicinity of the obstacle and do not radiate energy. Therefore, these trapped modes are of great physical importance because at the resonance frequencies, the response to a forced excitation can be quite high.

The case of real resonance frequencies ($\Im m(\omega) = 0$) has already been studied [1, 2]. These frequencies are obtained as eigenvalues of a self-adjoint operator. Due to the fluid-structure coupling, a quadratic eigenvalue problem is involved, in which the resonance frequencies ω solve the equations $\lambda(\omega) = \omega^2$ where λ are the eigenvalues of an operator of the form $A + \omega B$. Then the method is in two steps. For a fixed ω value, the spectrum of the operator is made of a continuous essential spectrum and of eigenvalues below the essential spectrum ($\omega < \omega_c$ defined in Eq. (6)). We restricted to the discrete spectrum which is studied thanks to the Min-Max principle. In particular we proved the existence of eigenvalues $\lambda_i(\omega)$, $i = 1, \cdots, N$ and we determined theoretical lower bounds for N. Then the fixed-point equations $\lambda_i(\omega) = \omega^2$, $i = 1, \cdots, N$ are solved. The number of resonances has been estimated versus various parameters, notably the flow velocity and the rigidity of the plate.

This study of real resonances has revealed an interesting behavior: when the fluid-structure problem is decoupled (rigid plate or fluid at rest), the resonance frequencies are necessarily real [1] (see also lemma 7). But when both effects are present, fluid in flow and elastic plate, the resonance frequencies can be complex [2]. This is the object of this paper, to study theoretically the resonance frequencies with $\Im m(\omega) > 0$. These complex frequencies are particularly interesting because they correspond to a stronger transient response to a source of frequency ω than for real frequencies: for a real resonance, the response varies like $te^{-i\omega t}$ whereas the response grows expo-

*

†POEMS, CNRS-INRIA-ENSTA UMR 7231, 828 Boulevard des Maréchaux, 91762 Palaiseau, France (jean-francois.mercier@ensta-paristech.fr).

This manuscript is for review purposes only.

nentially for a complex resonance, like $e^{\Im m(\omega)t}$. This latter case corresponds to the flutter instability encountered in aeroelasticity of airfoils [3, 4]. More generally the interaction of a finite flexible panel with a fluid flow with which the plate is aligned is a fundamental problem that has received a large attention because of its practical importance [5]. The main application lies in aerospace with the study of the airfoil flutter of a flexible plate immersed in an axial flow. This instability is similar to flag flutter and results from the competition between fluid forces and elasticity. The flutter instability has also applications in paper industry or snoring. Experimental [6] and numerical [7] studies have been carried out to clarify the paper flutter phenomenon, which currently limits the speed of printing machines and paper machines. Besides to study human snoring, the stability of a flexible cantilevered plate in channel flow has been studied as a representation of the dynamics of the human upper airway [8]. The focus is on instability mechanisms of the flexible plate that cause airway blockage during sleep. A last class of applications concerns nuclear engineering where parallel-plate assemblies are used as core elements in some nuclear research and power reactors. References on these subjects may be found in [9].

To our knowledge, this study is new. Most of the works on trapped modes concern a rigid body and a compressible fluid at rest [10, 11, 12], the main application being the water-waves trapped by vertical cylinders of various cross-section shapes. Unlike the case of an unbounded flexible wall [13], works on a bounded elastic body and a fluid in flow are rather focused on an incompressible flow [14] or a slightly compressible flow [15, 16, 17, 18]. Some studies consider the case of a compressible flow, but mostly for a membrane structure, not an elastic body, with applications to the control of noise [19, 20, 21]. The case of an elastic structure in a compressible flow has been treated but in conditions different from ours [22]: although we consider a rectangular geometry in the time-harmonic regime with an elastic plate clamped-free, in [22] is considered a cylindrical geometry in the time-domain with clamped-clamped boundary conditions. The configuration in [22] is a flow in a cylindrical tube, a portion of which is flexible: it is mostly a membrane and some results are given for a shell structure. Although these differences, a critical velocity U_c is defined in [22] to which we will compare (see paragraph 5.3). The critical velocity is derived using an alternative approach to ours, which consists in determining that a positive energy can be defined for $U < U_c$.

The outline of this paper is as follows. In the second section is presented the problem and the definition of what we call an instability is given. In the third section is derived a general criterion for the existence of instabilities and this criterion is precised in section 4: it is written in terms of the problem parameters, the ratio of densities μ, the flow velocity U and the ratio of sound speeds c. In particular, a volume in the space (μ, U, c) is defined such that no instabilities can develop in this volume. In section 5, the boundaries of this volume are further investigated. In particular, thanks to an approximation, threshold values μ_c and U_c are explicitly derived such that instabilities can develop only above these thresholds: $\mu > \mu_c$ and $U > U_c$. Finally, numerical validations of the derived theoretical estimates are presented in section 6.

2. The general framework.

2.1. Geometry and dimensional equations. The geometry is shown in Fig. 1: we consider the 2D waveguide $\tilde{\Omega} = \{(X, Y) \in \mathbb{R}\times]-h, h[\}$ filled with a compressible fluid. In the centre of the guide is placed an elastic plate $\tilde{\Gamma} = \{(X, Y), X \in]0, L[, Y = 0\}$. The fluid is in flow with a uniform velocity $u_0\boldsymbol{e}_X$. We take $0 < u_0 < c_0$ (subsonic flow) where c_0 is the uniform fluid sound speed.

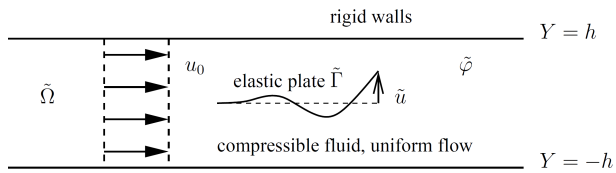

FIG. 1. *Geometry of the problem*

In time-harmonic regime of frequency $\tilde{\omega}$, if we send an incident wave $e^{i\tilde{\omega}(X/c_0-t)}$ from $X = -\infty$ on the plate and if we look for the scattered field, the problem is found well-posed except for a sequence of so-called resonance frequencies [1, 2]. These resonances correspond to the existence of eigenmodes (called also trapped modes): solutions in $L^2(\tilde{\Omega})$ of the problem without source. In this paper we focus on these trapped modes and therefore we look for a solution of the following homogeneous problem [1, 2]:

$$
\left\{
\begin{array}{l}
\left(\dfrac{\partial^2}{\partial X^2} + \dfrac{\partial^2}{\partial Y^2}\right)\tilde{\varphi} = \left(\dfrac{\tilde{D}}{c_0}\right)^2 \tilde{\varphi} \quad \text{in} \quad \tilde{\Omega}\backslash\tilde{\Gamma}, \\
\left(B\dfrac{d^4}{dX^4} - \rho_p h_p \tilde{\omega}^2\right)\tilde{u} = -[p](X,0) \quad \text{on} \quad \tilde{\Gamma}, \\
p(X,Y) = -\rho_a \tilde{D}\tilde{\varphi}(X,Y) \quad \text{in} \quad \tilde{\Omega}\backslash\tilde{\Gamma}, \\
\dfrac{\partial\tilde{\varphi}}{\partial Y}(X,0^{\pm}) = \tilde{D}\tilde{u} \quad \text{on} \quad \tilde{\Gamma}, \\
\dfrac{\partial\tilde{\varphi}}{\partial Y}(X,\pm h) = 0 \quad \text{for} \quad X \in \mathbb{R}, \\
\tilde{u}(0) = 0 = \tilde{u}'(0), \quad \tilde{u}''(L) = 0 = \tilde{u}'''(L),
\end{array}
\right. \tag{1}
$$

where p is the fluid pressure, $\tilde{\varphi}$ the fluid velocity potential and $\tilde{u}$ the vertical displacement of the plate. The velocity potential satisfies the convected Helmholtz equation whereas the displacement is solution of the linear plate equation. We have introduced $[p](X,0) = p(X,0^+) - p(X,0^-)$ the pressure jump through the plate and

$$\tilde{D} = u_0 \frac{\partial}{\partial X} - i\tilde{\omega},$$

the convective operator. The densities are ρ_a for the fluid (typically the air) and ρ_p for the plate. The plate of width h_p (supposed very small, the plate is seen as 1D) and of flexural rigidity B, is clamped at its leading edge $X = 0$ and free at its trailing edge $X = L$.

2.2. Some symmetries considerations. In the following we will restrict to an antisymmetric problem. Indeed, if the obstacle is symmetric and positioned symmetrically about the waveguide centerline, the solution can be decomposed into a symmetric and an antisymmetric part about that line. Antisymmetric trapped modes are generally looked for because the continuous spectrum of the antisymmetric solution has a nonzero lower limit given by the first duct cut-off frequency (see paragraph 2.4.4). Then the corresponding antisymmetric trapped modes can be found as discrete eigenvalues below the first cut-off frequency. On the contrary, for symmetric modes, all the spectrum is continuous.

Trapped modes can be determined if the obstacle is no longer symmetric about the waveguide centerline but this situation is mathematically more complicated. In

this case, possible discrete trapped mode frequencies are embedded in the continuous spectrum of the relevant operator, and one speaks of embedded trapped modes [23, 24, 25].

Since we only study antisymmetric modes, we can restrict to a half guide: $Y \in]0, h[$, the boundary condition $[p](X, 0)$ becomes $2p(X, 0)$ and the boundary condition $\tilde{\varphi}(X, 0) = 0$ for $X \notin [0, L]$ has to be added.

2.3. Dimensionless equations and reduction to a half guide. Following [9], we introduce the parameter γ such that

$$\gamma^2 = \frac{B}{\rho_p h_p},$$

and the following dimensionless parameters:

$$\alpha = \frac{h}{L}, \quad \mu = \frac{\rho_a L}{\rho_p h_p}, \quad c = c_0 \frac{L}{\gamma}.$$

α is an aspect ratio, μ compares the fluid and plate densities and c can be seen as the ratio of the fluid and plate sound speed. Following [9] we also introduce the dimensionless variables $x = X/L$, $y = Y/h$ and the following dimensionless quantities: velocity U, velocity potential φ, vertical plate displacement u and frequency ω defined by

$$u_0 = \frac{\gamma}{L} U, \quad \tilde{\varphi} = \gamma \varphi, \quad \tilde{u} = L u, \quad \tilde{\omega} = \frac{\gamma}{L^2} \omega.$$

We note $\Omega = \{(x, y) \in \mathbb{R} \times]0, 1[\}$ the half wave guide, $\Gamma = \{(x, y), x \in]0, 1[, y = 0\}$ the plate and $\Sigma = \{(x, y), x \in \mathbb{R}, y = 1\}$ the upper wall. Also we introduce $\Gamma^- = \{(x, y), x < 0, y = 0\}$ and $\Gamma^+ = \{(x, y), x > 1, y = 0\}$ (see Fig. 2) such that $\Gamma^- \cup \Gamma \cup \Gamma^+$ is the lower wall of the half-guide.

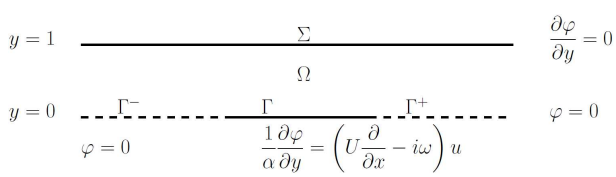

FIG. 2. *Geometry restricted to the half-guide*

Finally, the problem (1) written in a half waveguide in dimensionless form is

$$\left\{\begin{array}{rcl} \left(\dfrac{\partial^2}{\partial x^2} + \dfrac{1}{\alpha^2}\dfrac{\partial^2}{\partial y^2}\right)\varphi & = & \dfrac{1}{c^2}\left(U\dfrac{\partial}{\partial x} - i\omega\right)^2 \varphi \quad \text{in} \quad \Omega, \\ \left(\dfrac{d^4}{dx^4} - \omega^2\right) u & = & 2\mu\left(U\dfrac{\partial}{\partial x} - i\omega\right)\varphi(x, 0) \quad \text{on} \quad \Gamma, \\ \dfrac{1}{\alpha}\dfrac{\partial \varphi}{\partial y}(x, 0) & = & \left(U\dfrac{\partial}{\partial x} - i\omega\right) u \quad \text{on} \quad \Gamma, \\ \dfrac{\partial \varphi}{\partial y}(x, 1) & = & 0 \quad \text{on} \quad \Sigma, \\ \varphi(x, 0) & = & 0 \quad \text{on} \quad \Gamma^{\pm}, \\ u(0) = 0 = u'(0) & \text{and} & u''(1) = 0 = u'''(1). \end{array}\right. \tag{2}$$

This is a non-linear eigenvalue problem in which ω is the eigenvalue. As we will see, these eigenvalues can be divided in real and complex eigenvalues.

2.4. Some generalities on the trapped modes.

2.4.1. Definition of a resonance frequency. We are interested in the existence, for a complex frequency, of an acoustic field trapped around the plate, that we call a resonance:

Definition 1. *We say that*
$\omega \in \mathbb{C}$ *is a resonance frequency* $\Leftrightarrow \exists(\varphi, u) \in L^2(\Omega) \times L^2(\Gamma)$ *solution of* (2).
(φ, u) *is called the associated trapped mode.*

In practice it is more convenient to express the eigenproblem in a variational form. Thanks to the introduction of the functional spaces

$$V = \{\varphi \in H^1(\Omega), \varphi = 0 \quad \text{on} \quad \Gamma^{\pm}\}, \tag{3}$$

and

$$W = \{u \in H^2(\Gamma), u(0) = 0 = u'(0)\}, \tag{4}$$

and of the sequilinear form on $V \times W$:

$$b[(\varphi, u), (\psi, v)] = \int_\Omega (1 - M^2)\frac{\partial \varphi}{\partial x}\overline{\frac{\partial \psi}{\partial x}} + \frac{1}{\alpha^2}\frac{\partial \varphi}{\partial y}\overline{\frac{\partial \psi}{\partial y}} - i\frac{\omega}{c}M\left(\frac{\partial \varphi}{\partial x}\overline{\psi} - \varphi\overline{\frac{\partial \psi}{\partial x}}\right) + \frac{1}{2\mu\alpha}\int_\Gamma \frac{d^2u}{dx^2}\frac{d^2\overline{v}}{dx^2},$$

$$+ \frac{1}{\alpha}\int_\Gamma \overline{\psi}\left(U\frac{\partial u}{\partial x} - i\omega u\right) + \varphi\left(U\frac{\partial \overline{v}}{\partial x} + i\omega\overline{v}\right) - \omega^2\left(\frac{1}{c^2}\int_\Omega \varphi\overline{\psi} + \frac{1}{2\mu\alpha}\int_\Gamma u\overline{v}\right),$$

where we have introduced the Mach number $M \equiv U/c$, we can write the following equivalent variational formulation of the eigenvalue problem (2):

Definition 2. $\omega \in \mathbb{C}$ *is a resonance frequency* $\Leftrightarrow \exists(\varphi, u) \in V \times W$ *such that* $\forall(\psi, v) \in V \times W$, $b[(\varphi, u), (\psi, v)] = 0$.

We have three remarks:

- The space V plays the role of radiation conditions. Indeed away from the plate the velocity potential is decomposed on the duct modes, see Eq. (27) and more generally see Appendix A for the definition of the duct modes. Since the propagating modes are not in $H^1(\Omega)$, only the decreasing evanescent modes are selected when restricting to solutions in V, which leads to a solution trapped around the plate. In complement to the definition 2 corresponding to an unbounded domain, in Appendix A are defined the radiation conditions at finite distance which enables us to define in Appendix B the resonance problem set in a bounded domain. The equivalence between the two problems is also proved.
- The integration by parts leading to $b[(\varphi, u), (\psi, v)]$ involves the boundary term

$$-\left[\frac{U}{\alpha}\varphi\overline{v}\right](1, 0).$$

  We have imposed a Kutta condition at the trailing edge of the plate: we have set this term to zero by assuming that the condition $\varphi(x > 1, 0) = 0$ can be extended by continuity to $x = 1$. Another classical Kutta condition is to impose the fluid velocity to be finite at the plate trailing edge. This requires to use sophisticated tools like a Wiener-Hopf approach [26, 27] and makes our analysis method inapplicable. The choice of the right Kutta condition is

important since such choice has been proved to have strong influence on the far-field, in particular on the upstream radiation pattern [26]. But it seems to have a reduced influence on the unstable frequencies we are studying. Indeed we have compared our results to the results in [27], in which only a rigid plate in a flow is considered. We have found for different flow velocities that when changing the Kutta condition from ours to the finite velocity one, the resonance frequencies are just slightly moved in the complex plane. Even though only the case of a rigid plate and a particular α value have been tested, we assume that it is a general behavior: when changing of Kutta condition, the resonance frequencies only slightly move in the complex plane.

- written back with dimensional quantities, $M = u_0/c_0$ and thus $M < 1$ since the flow is supposed subsonic.

2.4.2. Properties of the resonance frequencies. The search of ω in the complex plane can be restricted to a fourth of the complex plane since the spectrum of resonance frequencies has some nice properties:

LEMMA 3. *If ω is an eigenvalue of (2), then $-\omega$ and $\pm\overline{\omega}$ are also eigenvalues.*

Proof. By taking the complex conjugated of (2), we deduce immediately that if ω is an eigenvalue associated to the eigenmode (φ, u) then so is $-\overline{\omega}$ simply associated to $(\overline{\varphi}, \overline{u})$.

The other property that if ω is an eigenvalue then so is $\overline{\omega}$ is mode delicate to obtain. In Appendix B we give the proof for the continuous mathematical problem. The proof is rather technical and requires to restrict the resonance problem to a bounded domain to get compacity properties in order to use the Fredholm alternative.

An alternative proof is given here, easier but restricted to the discretized problem. We have determined numerically the resonance frequencies thanks to a method coupling Finite Elements and a modal expansion. The velocity potential is discretized on a Finite Element basis while the plate displacement is expanded on the modes of the plate (details in Appendix C). This leads to a matricial problem to solve of the form

$$(A + i\omega B + \omega^2 C)X = 0, \tag{5}$$

where A, B and C are Finite Element matrices and X is a vector concatenating the nodal values of φ and the modal components of u. A, B and C are real valued matrices with A and C symmetric and B antisymmetric. Then we can prove that if ω is an eigenvalue, $-\omega$ is also an eigenvalue. Indeed ω is an eigenvalue is equivalent to $\det(A + i\omega B + \omega^2 C) = 0$. Then using that for any matrix M we have $\det(M) = \det(M^T)$, we get that $\det(A - i\omega B + \omega^2 C) = 0$. Finally, we have proved that if ω is an eigenvalue then $-\overline{\omega}$ and $-\omega$ are also eigenvalues. But then, since $-\omega$ is an eigenvalue, $\overline{\omega}$ and ω and are also eigenvalues which ends the proof. ∎

2.4.3. An example of resonances. To show the complexity of the behaviors of the resonance frequencies versus the various parameters of the problem, we present here a typical example of such behavior. The non-linear eigenvalue problem (5) can be written as a classical (but generalized) eigenvalue problem: noting $Y = \omega X$, we get:

$$\begin{pmatrix} 0 & 1 \\ A & iB \end{pmatrix} \begin{pmatrix} X \\ Y \end{pmatrix} = \omega \begin{pmatrix} 1 & 0 \\ 0 & -C \end{pmatrix} \begin{pmatrix} X \\ Y \end{pmatrix}.$$

As proved in the previous paragraph, the search of ω in the complex plane can be restricted to a fourth of this plane: we just represent the eigenvalues in the quarter

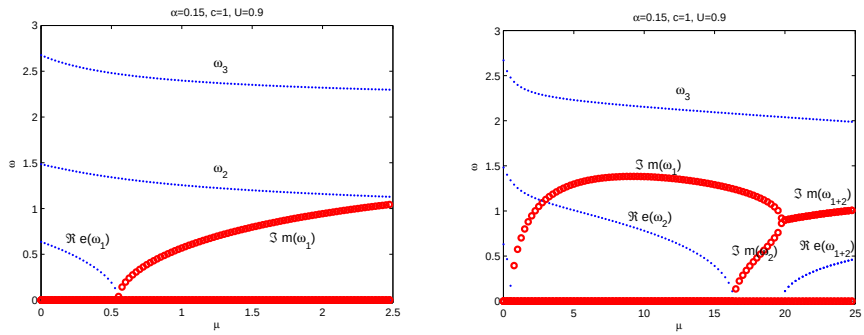

FIG. 3. *Three lowest resonance frequencies ω when μ varies for $\alpha = 0.15$, $c = 1$ and $U = 0.9$. $\Re e(\omega)$ with dots and $\Im m(\omega)$ with circles. (a): zoom on the small μ values, up to 2.5, (b): $0 < \mu < 25$*

plane $\Re e(\omega) \geq 0$, $\Im m(\omega) \geq 0$. In Fig. 3 are plotted the evolution of the three lowest (in the sense $|\omega|$ small) resonance frequencies when μ varies, the other parameters being fixed: $c = 1$ and $U = 0.9$. In all the figures of this paper, we fix the geometry and we take $\alpha = 0.15$ which corresponds to a plate of length $L \approx 7h$. The real parts of ω are with dots and the imaginary parts are with circles. Fig. 3(b) is for $0 < \mu < 25$ whereas Fig. 3(a) corresponds to a zoom on the small μ values, up to 2.5. We see in Fig. 3(a) that for small values of μ (here $\mu < \mu_c \equiv 0.55$) all the frequencies are real. At the threshold μ_c, the first frequency ω_1 vanishes and is found to turn from purely real to purely imaginary. As we will detail latter, it becomes an instability. In Fig. 3(b), we see that at $\mu = 16.4$, the second real frequency ω_2 becomes purely imaginary, leading to a second instability for $\mu > 16.4$. Moreover, an interesting event happens at $\mu = 19.9$, illustrating the complexity of the resonances behavior and showing also that the complex frequencies are not necessarily associated to a zero real part: the two instabilities, purely imaginary, merge to create for $\mu > 19.9$ a complex frequency ω_{1+2} with non-zero real and imaginary parts. In this paper, we will focus on the first threshold μ_c and we will characterize it: we will derive a lower bound of this threshold value and also we will find an upper bound of the modulus of the first unstable frequency (an upper bound of the red curves in Fig. 3).

From Fig. 3, it appears that the resonances can be divided in two classes:

DEFINITION 4. *Let $\omega \in \mathbb{C}$ be a resonance frequency (definition (2)).*
- $\Im m(\omega) = 0 \Rightarrow \omega$ *is called a real resonance,*
- $\Im m(\omega) > 0 \Rightarrow \omega$ *is called an instability.*

We will now give some properties of these two kind of resonances.

2.4.4. The real resonance frequencies. The study of real frequencies has already been done [1, 2] . They have been looked for below the cut-off frequency ω_c of the half wave-guide (with a Dirichlet boundary condition at $y = 0$, see Appendix A)

$$\omega < \omega_c \equiv \frac{\pi}{2\alpha}\sqrt{c^2 - U^2}. \tag{6}$$

Indeed, only a finite number of eigenfunctions, so-called propagating modes, propagate undamped along the waveguide while all other so-called evanescent modes decay [28]. Only the propagating modes can radiate energy to infinity and below the cut-off frequency ω_c, all the guided modes are evanescent (see Appendix A). Then the velocity

potential φ, which away from the plate can be decomposed on the guided modes, naturally decreases exponentially when $|x| \to \infty$: it is localized around the plate and thus called a trapped mode.

Above the cut-off frequency, some resonance frequencies may exist, but they are embedded in the continuous spectrum and their mathematical study is much more involved [23, 24, 25].

2.4.5. The instabilities. We consider causal solutions and thus we focus on the asymptotic solutions behavior only when $t \to \infty$. The second case $\Im m(\omega) > 0$ corresponds to an unstable behavior since $e^{-i\omega t} = e^{-i\Re e(\omega)t} e^{\Im m(\omega)t}$ and $e^{\Im m(\omega)t} \to \infty$ when $t \to \infty$ (we do not restrict when considering that $\Im m(\omega) > 0$ since if ω is a resonance frequency, $\overline{\omega}$ is also a resonance frequency).

Note that these unstable frequencies are not the usual "complex resonances" that have been studied for rigid bodies [29, 30] or elastic bodies [31, 32]. The complex resonances are defined as the poles of the analytical continuation of the resolvent scattering operator and are also called scattering frequencies. These poles are very different from the unstable frequencies: the associated modes are not trapped but on the contrary they grow far from the scattering body. These modes are called leaky modes since they have radiation losses. Moreover the analytical continuation is made in the half plane $\Im m(\omega) < 0$ which corresponds to a decreasing behavior in time. Therefore the leaky modes cannot correspond to instabilities.

To sum up:

- a complex resonance is bounded in time but not bounded in space,
- an instability is bounded in space but not bounded in time.

In the rest of the paper, to avoid confusion, we will talk about instabilities and not complex resonances and we will focus on the existence conditions of these instabilities.

3. General results on the instability frequencies. First we give general properties on the imaginary part of a resonance frequency.

LEMMA 5. *If ω is a resonance frequency and if (φ, u) is the associated trapped mode, then $\Im m(\omega) a(\omega; \varphi, u) = 0$ where*

$$a(\omega; \varphi, u) = \int_\Omega (1 - M^2) \left| \frac{\partial \varphi}{\partial x} \right|^2 + \frac{1}{\alpha^2} \left| \frac{\partial \varphi}{\partial y} \right|^2 + \frac{1}{2\mu\alpha} \int_\Gamma \left| \frac{d^2 u}{dx^2} \right|^2 \tag{7}$$

$$+ \frac{2U}{\alpha} \Re e \int_\Gamma \overline{\varphi} \frac{\partial u}{\partial x} + |\omega|^2 \left(\frac{1}{c^2} \int_\Omega |\varphi|^2 + \frac{1}{2\mu\alpha} \int_\Gamma |u|^2 \right).$$

Proof. From definition 2, taking $(\psi, v) = (\varphi, u)$, the result is deduced using

$$\Im m \left\{ -\frac{1}{\omega} b[(\varphi, u), (\varphi, u)] \right\} = 0.$$

∎

This lemma has a simple consequence: a general non-existence result for instabilities, that will be used in all the following of the paper.

LEMMA 6. *If $\forall (\varphi, u) \in V \times W$, $a(\omega; \varphi, u) > 0$, then ω cannot be an instability.*

Proof. This is a consequence of lemma 5 and definition 4: $\Im m(\omega) a(\omega; \varphi, u) = 0$ and $a(\omega; \varphi, u) > 0$ implies $\Im m(\omega) = 0$.

REMARK 1. *In this paper we derive non-existence results for instabilities and we do not know how to derive an existence result for instabilities. But since in practice*

we wish to avoid instabilities, it is useful to determine in which conditions we are sure they do not develop.

REMARK 2. *We do not discuss if the instabilities we look for are physical (in the sense causal) solutions. The boundary conditions are assumed to be decay at infinity for any $\Im m(\omega)$, and this is definitely correct for the case we are interested in of $\Im m(\omega) > 0$, but may not be physically correct or causal for the other solutions with $\Im m(\omega) < 0$, in particular if $\Im m(\omega)$ is sufficiently negative. This causality question is complicated when considering complex frequencies but hopefully not essential for us since we focus on cases for which no instabilities can exist, whether they are causal or not. If we wanted to describe how to excite an instability, then the causality question would become essential.*

In the rest of the paper, we will derive simple conditions on the parameters of the problem under which lemma 6 is fulfilled.

4. Criteria of non-existence of instabilities. Following lemma 6, for a fixed frequency ω we look now for conditions, as simple as possible, for which $a(\omega;\varphi,u) > 0$, $\forall(\varphi,u) \in V \times W$.

4.1. A simple criterion. A first result is, as announced in the introduction, that only the joint effects of the elasticity of the plate and of the flow can create instabilities:

LEMMA 7. *If the fluid is at rest ($U = 0$) or the plate rigid ($u = 0$), there is no instability.*

Proof. In the expression of $a(\omega;\varphi,u)$ in (7), all the terms are strictly positive for $(\varphi,u) \neq (0,0)$ excepting the term

$$\frac{2U}{\alpha}\Re e \int_\Gamma \overline{\varphi}\frac{\partial u}{\partial x}. \qquad \square$$

Therefore, if this term is equal to zero, there is no instability using lemma (6). This is the case if $U = 0$ or $u = 0$.

As already said, the trapped modes for these uncoupled problems (fluid at rest or rigid plate) have already been studied [1]. In this paper we focus on instabilities.

4.2. A general criterion. We will now state the main theorem of this paper, giving an explicit sufficient condition to have no instability. For this theorem, we need to introduce some notations. We introduce

$$\lambda_1 = \inf_{\varphi \in V\setminus\{0\}} R(\varphi), \tag{8}$$

where we have introduced the Rayleigh quotient

$$R(\varphi) = \frac{\int_\Omega (c^2 - U^2)\left|\frac{\partial\varphi}{\partial x}\right|^2 + \frac{c^2}{\alpha^2}\left|\frac{\partial\varphi}{\partial y}\right|^2}{\int_\Omega |\varphi|^2}. \tag{9}$$

Also we introduce

$$\alpha_1^4 = \inf_{u \in W\setminus\{0\}} \frac{\int_\Gamma \left|\frac{d^2u}{dx^2}\right|^2}{\int_\Gamma |u|^2}. \tag{10}$$

The values λ_1 and α_1^4 are the first eigenvalues of problems that are specified in Appendix D. The value λ_1 is sometimes called the first eigenvalue of vibration for the fluid [22]. Its value is determined numerically and a useful approximation of λ_1 is derived in Appendix D. In Eq. (10), $\alpha_1^2 = \omega_1^{\text{plate}}$ where ω_1^{plate} is the first eigenfrequency of the plate alone in vacuum. Numerically it is found that $\alpha_1 = 1.88$.

Finally we introduce

$$\hat{\sigma} \equiv \min\left(\lambda_1, \alpha_1^4\right), \tag{11}$$

and

$$\beta = \frac{\alpha}{c}\sqrt{\hat{\sigma}}. \tag{12}$$

With these notations, we have the

THEOREM 8. *Let*

$$T(\omega) \equiv \hat{\sigma}\left[1 - U\left(\frac{2}{\beta} + \beta\right)\sqrt{\alpha\mu}\right] + |\omega|^2, \tag{13}$$

where $\hat{\sigma}$ and β are defined in (11) and (12). If $T(\omega) > 0$, then ω cannot be an instability.

Proof. The idea is to show that $T(\omega)$ is a lower bound of $a(\omega;\varphi,u)$ and then to use lemma 6. In this aim, first we derive a general lower bound for a, depending on some parameters obtained only numerically. Second, we derive another lower bound, a little less accurate, but given in a closed-form and thus easier to utilise.

• a general lower bound for $a(\omega;\varphi,u)$

We decompose a defined in (7) in three parts: $a = a_1 + a_2 + a_3$, with

$$\begin{cases} a_1(\varphi,u) = \displaystyle\int_\Omega (1-M^2)\left|\frac{\partial\varphi}{\partial x}\right|^2 + \frac{1}{\alpha^2}\left|\frac{\partial\varphi}{\partial y}\right|^2 + \frac{1}{2\mu\alpha}\int_\Gamma \left|\frac{d^2u}{dx^2}\right|^2, \\ a_2(\varphi,u) = \displaystyle\frac{2U}{\alpha}\Re e\int_\Gamma \overline{\varphi}\frac{\partial u}{\partial x}, \\ a_3(\varphi,u) = |\omega|^2||(\varphi,u)||^2, \end{cases} \tag{14}$$

with

$$||(\varphi,u)||^2 = \frac{1}{c^2}\int_\Omega |\varphi|^2 + \frac{1}{2\mu\alpha}\int_\Gamma |u|^2.$$

We look for a positive lower bound for a and in this aim, we determine a small upper bound for $|a_2|$. Using the Poincaré's inequality it is found that $\forall u \in W$ defined in (4)

$$\int_\Gamma \left|\frac{du}{dx}\right|^2 \leq \frac{1}{2}\int_\Gamma \left|\frac{d^2u}{dx^2}\right|^2. \tag{15}$$

We also use the trace inequality: $\forall\tau > 0$ and $\forall\varphi \in V$,

$$\int_\Gamma |\varphi|^2 \leq (1+\tau^2)\int_\Omega |\varphi|^2 + \frac{1}{\tau^2}\int_\Omega \left|\frac{\partial\varphi}{\partial y}\right|^2. \tag{16}$$

This trace inequality is derived by using an alternative of the Poincaré's inequality for a fixed value of x, and then by integrating along the x axis on the plate Γ.

Then, writing a_2 under the form

$$a_2 = 2\eta \int_\Gamma \frac{\tau}{\alpha} |\varphi| \frac{\left|\frac{du}{dx}\right|}{\sqrt{\mu\alpha}},$$

with $\eta = U\sqrt{\mu\alpha}/\tau$, we deduce with Young's inequality and then with (15) and (16) that:

$$\begin{aligned}\frac{|a_2|}{\eta} &\leq \int_\Gamma \frac{\tau^2}{\alpha^2} |\varphi|^2 + \frac{1}{\mu\alpha} \left|\frac{du}{dx}\right|^2, \\ &\leq \frac{\tau^2(1+\tau^2)}{\alpha^2} \int_\Omega |\varphi|^2 + \frac{1}{\alpha^2} \int_\Omega \left|\frac{\partial\varphi}{\partial y}\right|^2 + \int_\Gamma \frac{1}{2\mu\alpha} \left|\frac{d^2u}{dx^2}\right|^2.\end{aligned}$$

Then using (14) leads to

$$\frac{|a_2|}{\eta} \leq \tau^2(1+\tau^2)\frac{c^2}{\alpha^2}||(\varphi,u)||^2 + a_1.$$

Finally, using $a \geq a_1 - |a_2| + a_3$, we deduce $\forall(\varphi,u) \in V \times W$, $(\varphi,u) \neq (0,0)$ and $\forall\omega \in \mathbb{C}$:

$$\frac{a(\omega;\varphi,u)}{||(\varphi,u)||^2} \geq (1-\eta)\sigma^\star - \eta\tau^2(1+\tau^2)\frac{c^2}{\alpha^2} + |\omega|^2,$$

where

$$\sigma^\star = \inf_{(\varphi,u)\in V\times W} \frac{a_1(\varphi,u)}{||(\varphi,u)||^2}.$$

This lower bound is more accurate than T defined in (13) but requires the use of some numerics to determine $\sigma^\star$. To find the closed-form formula (13), we need to evaluate a more explicit lower bound for $\sigma^\star$, noted $\hat{\sigma}$ and also to choose the value of τ.

- an explicit lower bound for $a(\omega;\varphi,u)$

◦ Value of $\hat{\sigma}$

The value of $\hat{\sigma}$ is obtained by using the inequality for any positive real numbers a, b, c and d:

$$\frac{a+b}{c+d} \geq \min\left\{\frac{a}{c}, \frac{b}{d}\right\},$$

from which is deduced $\forall(\varphi,u) \in V \times W$, $(\varphi,u) \neq (0,0)$

$$\frac{a_1(\varphi,u)}{||(\varphi,u)||^2} \geq \min\left\{\frac{\int_\Omega (c^2-U^2)\left|\frac{\partial\varphi}{\partial x}\right|^2 + \frac{c^2}{\alpha^2}\left|\frac{\partial\varphi}{\partial y}\right|^2}{\int_\Omega |\varphi|^2}, \frac{\int_\Gamma \left|\frac{d^2u}{dx^2}\right|^2}{\int_\Gamma |u|^2}\right\},$$

which leads to

$$\sigma^\star \geq \hat{\sigma} \equiv \min\left(\lambda_1, \alpha_1^4\right),$$

using the definitions (8) and (10). Finally we get

$$\frac{a(\omega;\varphi,u)}{||(\varphi,u)||^2} \geq T,$$

with T defined by

$$T = \hat{\sigma} - \frac{U}{\tau}\sqrt{\mu\alpha}\left[\hat{\sigma} + \tau^2(1+\tau^2)\frac{c^2}{\alpha^2}\right] + |\omega|^2.$$

∘ Value of τ

To get (13), the value of τ has to be chosen. If $U = 0$, $T(\omega) = \hat{\sigma} + |\omega|^2$ is always positive and we recover that all the resonances are real for a fluid at rest (lemma 7). For $U > 0$, we choose τ such that T remains positive as long as possible when U increases. It means that we need

$$\frac{\hat{\sigma} + \tau^2(1+\tau^2)\dfrac{c^2}{\alpha^2}}{\tau},$$

to be small. It is straightforward to check that this quantity is minimum for $\tau = \hat{\beta}$ with

$$\hat{\beta}^2 = \frac{1}{6}\left(-1 + \sqrt{1 + 12\frac{\hat{\sigma}\alpha^2}{c^2}}\right). \tag{17}$$

□

If $\hat{\sigma}\alpha^2/c^2$ is large, we get the approximation $\hat{\beta}^2 \simeq \hat{\sigma}\alpha^2/c^2$. We have checked numerically that $\hat{\sigma}\alpha^2/c^2$ remains a good approximation of $\hat{\beta}^2$, even when it is not large (see Fig. 4). Therefore we choose to define τ by the value of β in(12) which leads to the expression (13) of T.

A nice consequence of Theorem (8) is that we can establish a closed-form criterion for the appearance of instabilities. This is done in the next paragraph.

4.3. A threshold for instabilities existence. Utilizing theorem 8, we can deduce a threshold for the possible existence of an instability and also a bounding of the modulus of the unstable frequencies above the threshold. If we introduce the function

$$f(\mu, U, c) = U\left(\frac{2}{\beta} + \beta\right)\sqrt{\alpha\mu}, \tag{18}$$

we have the

Corollary 9. *A resonance frequency ω is necessarily real if*

- $f(\mu, U, c) < 1$,
- $f(\mu, U, c) \geq 1$ *and* $|\omega|^2 > \hat{\sigma}\,[f(\mu, U, c) - 1]$.

In other words, an instability ω can exist only if $f(\mu, U, c) > 1$ and $|\omega|^2 \leq \hat{\sigma}\,[f(\mu, U, c) - 1]$.

Remark 3. *When it exists, an instability ω is necessarily of small modulus $|\omega|$ since ω is located in the complex plane $(\Re e(\omega), \Im m(\omega))$ inside a disc of bounded radius $R = \sqrt{\hat{\sigma}\,[f(\mu, U, c) - 1]}$.*

Proof. This corollary is a direct consequence of theorem 8:

$$T(\omega) > 0 \Rightarrow \Im m(\omega) = 0.$$

□

The improvement of corollary 9, compared to theorem 8, is that the conditions leading to $T > 0$ have been written in a closed-form.

Although this corollary is rather explicit, it is not so easy to use in practice because it describes the joint effects of μ, U and c. Before presenting numerical validations of the theoretical estimates, in the next section we will simplify corollary 9 by considering separately the different effects.

5. Analysis of the stability area. The previous corollary has introduced a "stability area", defined by

$$f(\mu, U, c) < 1. \tag{19}$$

It corresponds to an unbounded volume in the space (U, μ, c) in which no instability can exist and we will now characterize this volume. This volume can be obtained numerically (see Fig. 7) but we wish here to get closed-form results, easier to utilise. To do so, an approximation is required: in Appendix D we prove that λ_1 defined in (8) can be approximated by $\lambda_1 \simeq (c^2 - U^2)\pi^2$. Thus $\hat{\sigma}$ defined in (11) can be approximated by

$$\sigma = \min\left[(c^2 - U^2)\pi^2, \alpha_1^4\right]. \tag{20}$$

Since β defined in (12) depends on U and c, the dependence of the volume defined in (19) versus U or c is rather involved. On the contrary, the dependence versus μ is explicit: f is an increasing function of μ and the relation (19) is obviously not fulfilled for large μ values. For its simplicity, we start by analyzing the dependence versus μ.

5.1. Influence of μ. μ becomes large when the fluid is heavy and/or the plate is light and this is necessary for the possible development of instabilities as stated in the following lemma:

LEMMA 10. *For U and c fixed, an instability ω can exist only if*

- $\mu > \mu_c$,
- $|\omega|^2 < \hat{\sigma} U \left(\frac{2}{\beta} + \beta\right) \sqrt{\alpha}\left(\sqrt{\mu} - \sqrt{\mu_c}\right)$, *where the critical threshold μ_c is defined by*

$$\mu_c = g(U, c) \equiv \frac{1}{\alpha U^2 \left(\frac{2}{\beta} + \beta\right)^2} \tag{21}$$

Proof. f defined in (18) is obviously an increasing function of μ. Therefore, if we define μ_c by $f(\mu_c, U, c) = 1$ which is equivalent to (21), we deduce that

$$\mu < \mu_c \Leftrightarrow f(\mu, U, c) < 1.$$

Then the lemma is just a consequence of Corollary (9). ∎

The validity of this lemma is illustrated in Fig. 4, where are represented the three first resonance frequencies when μ varies for $\alpha = 0.15$, $c = 1$ and $U = 0.7$. $\Re e(\omega)$ is represented with dots and $\Im m(\omega)$ with circles. Using (6), the cut-off frequency is $\omega_c = 7.48$. Two additional curves represent the function

$$h : \begin{cases} \mu \to 0 \quad \text{for} \quad \mu < \mu_c, \\ \mu \to \sqrt{\hat{\sigma} U \left(\frac{2}{\beta} + \beta\right) \sqrt{\alpha}\left(\sqrt{\mu} - \sqrt{\mu_c}\right)} \quad \text{for} \quad \mu > \mu_c, \end{cases} \tag{22}$$

where $\mu_c = 0.35$ is determined with (21). The difference between the two curves is the value of σ and of β: the straight line is an approximated curve evaluated with (20) and (12) whereas the dashed line is exact and corresponds to the use of (11) and (17). As announced previously, (20) and (12) are confirmed to be very good approximations of (11) and (17).

Fig. 4 validates Lemma 10: the instability develops for values of $\mu > 2$, larger than μ_c and the modulus of the unstable frequency (here $|\Im m(\omega_1)| = |\omega_1|$ since $\Re e(\omega_1) = 0$ for the instability) is below the solid and dashed curves.

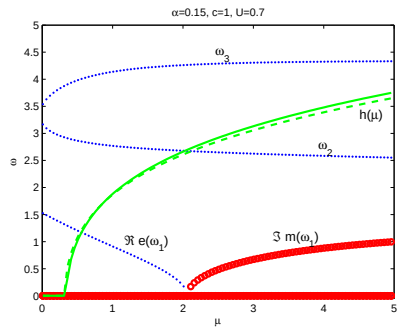

FIG. 4. *Three lowest resonance frequencies ω_n, $n = 1, 2$ and 3 when μ varies for $\alpha = 0.15$, $c = 1$ and $U = 0.7$. $\Re e(\omega)$ with dots and $\Im m(\omega)$ with circles. Upper boundary $h(\mu)$ for $|\omega|$, defined in (22): solid line for the approximated boundary and dashed line for the exact one*

5.2. Influence of U and c. We study now how varies f versus U and c. To simplify the study and get monotonous behaviors, we restrict ourselves to the case $\alpha\pi < \sqrt{2}$ which means that the plate is long enough ($\sqrt{2}L > \pi h$).

LEMMA 11. *For $\alpha\pi < \sqrt{2}$, $f(\mu, U, c)$ is an increasing function of U and for values of c such that $c < \alpha_1^2/\pi$, f is a decreasing function of c. In other words, an instability can occur only for U large enough or c small enough.*

Proof. We note $\theta(x) = \dfrac{2}{x} + x$ such that f in (18) is defined by

$$f(\mu, U, c) = U\theta(\beta)\sqrt{\alpha\mu}. \qquad \square$$

Recalling that there is no instability if $f(\mu, U, c) < 1$, we need to evaluate β from (12) to conclude. The results depend on the value of $\sigma = \min\left[(c^2 - U^2)\pi^2, \alpha_1^4\right]$ and thus on the sign of $U^2 + \dfrac{\alpha_1^4}{\pi^2} - c^2$:

- If $c^2 < U^2 + \dfrac{\alpha_1^4}{\pi^2}$, then $\sigma = (c^2 - U^2)\pi^2$ and thus $\beta = \alpha\pi\sqrt{1 - M^2}$
- If $c^2 > U^2 + \dfrac{\alpha_1^4}{\pi^2}$, then $\sigma = \alpha_1^4$ and thus $\beta = \dfrac{\alpha_1^2\alpha}{c} < \alpha\pi\sqrt{1 - M^2}$

Therefore, in all cases, $\beta \leq \alpha\pi$. Now we use the fact that θ is decreasing for $x < \sqrt{2}$. Therefore, if $\alpha\pi < \sqrt{2}$, $\theta(\beta)$ is a decreasing function of β. The conclusion is then easy to deduce: $f \nearrow$if

- $U \nearrow$,
- $c^2 < U^2 + \dfrac{\alpha_1^4}{\pi^2}$ and $c \searrow$
- $c^2 > U^2 + \dfrac{\alpha_1^4}{\pi^2}$ and $c \nearrow$.

In particular, if $c < \alpha_1^2/\pi$, $f \nearrow$ when $c \searrow$.

To illustrate this lemma, we have represented in Fig. 5 isovalues of the function $g(U, c)$ defined in (21). The black thick line is the curve $c^2 = U^2 + \alpha_1^4/\pi^2$, which corresponds to the change of definition for σ (see (20)). We recall that we have two equivalent definitions for the stability area:

$$f(\mu, U, c) < 1 \Leftrightarrow \mu < g(U, c).$$

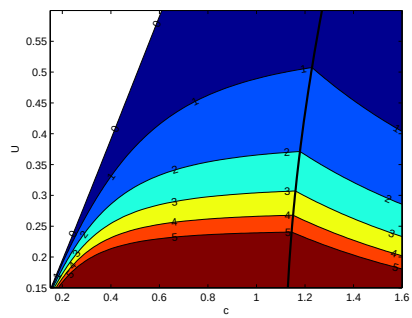

FIG. 5. *Isovalues of the function $g(U,c)$ defined in (21) for $\alpha = 0.15$. For $\mu = \mu_0$, the area $g(U,c) > \mu_0$ in the (U,c) plane is stable. Curve $c^2 = U^2 + \alpha_1^4/\pi^2$ in black thick line*

Therefore, if $\mu = \mu_0$, the stability zone is defined by the area in the (U,c) plane such that $g(U,c) > \mu_0$. Values of μ_0 between 1 and 5 are indicated in Fig. 5. We see that this area reduces when μ increases. We see also that we go out the stability zone when increasing U or μ or decreasing c if $c < \alpha_1^2/\pi$, in accordance with lemma 11.

Contrary to the simple dependence versus μ, it is not possible to define, starting from (19), closed-form critical threshold U_c and c_c such that an instability can occur only for $U > U_c$ or $c < c_c$. However, by approximating (19), it is possible to derive an approximate value of U_c, noted U_c^{app}, which compares with the one derived in [22].

5.3. Simplifications for the influence of U. Still for $\alpha\pi < \sqrt{2}$, since $f(\mu, U, c)$ is an increasing function of U, we can introduce the threshold frequency U_c defined by

$$f(\mu, U_c, c) = 1. \tag{23}$$

Let us recall that thanks to lemma 11 we have the following alternative:

- If $U < U_c \Rightarrow$ no instabilities exist
- If $U > U_c \Rightarrow$ instabilities can exist

The aim of this paragraph is to look for a closed-form expression of U_c, as obtained in [22]. We have

LEMMA 12. *For $\alpha\pi < \sqrt{2}$ and $c < \alpha_1^2/\pi$, $U_c < U_c^{app}$ where*

$$(U_c^{app})^2 = \frac{\alpha\pi^2 c^2}{4\mu c^2 + \alpha\pi^2}, \tag{24}$$

and U_c is defined in (23).

Proof. The condition on c implies, from (20), that $\hat{\sigma} = (c^2 - U^2)\pi^2$. Then we introduce an approximation of f, deduced by cancelling the term β in (18). It is thus defined by

$$f^{\text{app}}(\mu, U, c) = U\frac{2}{\beta}\sqrt{\alpha\mu} = \frac{2}{\pi}\sqrt{\frac{\mu U^2 c^2}{\alpha(c^2 - U^2)}},$$

□

and it is such that $f^{\text{app}} < f$. To this approximated function is associated an approximated threshold velocity U_c^{app}, defined by $f^{\text{app}}(\mu, U_c^{\text{app}}, c) = 1$. It leads to (24) which is similar to the value in [22] (4 is replaced by 1 in [22], leading to a less precise upper bound, certainly due to a 1D approximation of the acoustic propagation introduced

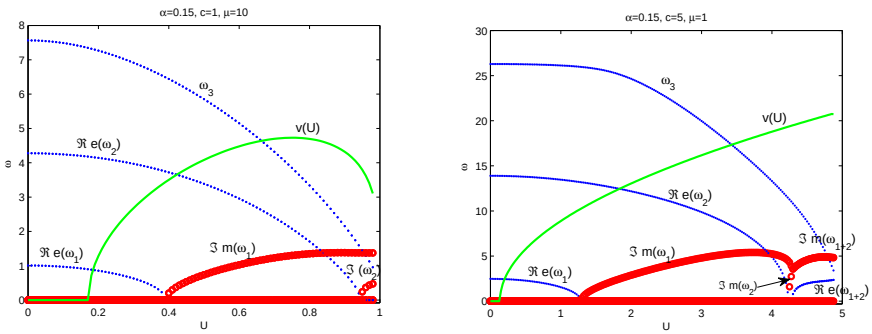

FIG. 6. *Three lowest resonance frequencies ω_n, $n = 1, 2, 3$ when U varies for $\alpha = 0.15$. $\Re e(\omega)$ with dots and $\Im m(\omega)$ with circles. Upper boundary $v(U)$ for $|\omega|$, defined in (25), in solid line. (a) $c = 1$ and $\mu = 10$, (b) $c = 5$ and $\mu = 1$*

in [22]). Finally, U_c^{app} is less precise than U_c since it is an upper bound for U_c: indeed $f^{\text{app}} < f$ and f^{app} is an increasing function of U.

6. Numerical validation of the estimates. The aim of the numerical study is mostly to validate corollary 9. First we look the influence of the velocity U. Then we illustrate the validity of the stability area defined in (19).

6.1. Threshold for the velocity. In Fig. 6 are plotted the three first resonance frequencies when U varies between 0 and c for $\alpha = 0.15$ and for two values of (c, μ). $\Re e(\omega)$ is represented with dots and $\Im m(\omega)$ with circles. The green curves represent the function

$$v : U \to \sqrt{\max\left\{0, \sigma\left[U\left(\frac{2}{\beta} + \beta\right)\sqrt{\alpha\mu} - 1\right]\right\}}, \tag{25}$$

involved in corollary 9 with σ and β evaluated thanks to (20) and (12). Corollary 9 asserts that an instability ω can not exist if $v(U) = 0$ and that, when it exists, it must satisfy

$$|\omega| \leq v(U).$$

These results are validated since the circles are found below the continuous solid curves. Note that in Fig. 6(b), at $\mu = 4.3$, two purely imaginary frequencies merge to produce a frequency ω_{1+2} with non-zero real and imaginary parts for $\mu > 4.3$ (as in Fig. 3(b)). The modulus of the complex frequency ω_{1+2} is not represented but it is clearly below the values of the green curve.

6.2. Stability area. Now we focus on the shape of the stability area, defined by (19), $f(\mu, U, c) < 1$, versus μ, U and c. Lemmas 10 and 11 indicate that the stability area corresponds to μ or U small enough (the behavior versus c is more involved). In other words, we expect instabilities to appear when increasing μ or U. We will see numerically that it is the case and that instabilities only develop outside the stability area, confirming the validity of the theoretical estimates. In Fig. 7 are plotted two isovalues of the function $f(\mu, U, c)$ defined in (18) for $\alpha = 0.15$ and with one parameter fixed: Fig. 7 (a) is for $c = 1$ and Fig. 7 (b) for $\mu = 1$. The isovalue $f(\mu, U, c) = 1$ is represented to show the borderline of the theoretical stability area. The isovalue $f = 2$ is included to clarify the location of the theoretical stability area $f(\mu, U, c) < 1$ (it is

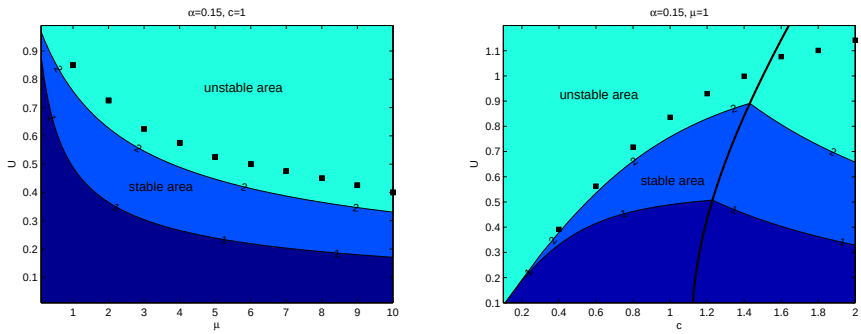

FIG. 7. *Isovalues of* $f(\mu, U, c)$ *defined in* (18) *for* $\alpha = 0.15$. *(a)* $c = 1$, *(b)* $\mu = 1$.

enough since f has monotonous variations). The black squares represent the couple of values obtained numerically, (μ, U) or (c, U), for which an instability appears. It means that the area above the black squares is an unstable area associated with the effective existence (found numerically) of instabilities. Fig. 7 confirms that the lower area $f(\mu, U, c) < 1$ (in dark) corresponds to a stability area since the black squares are outside this area. Note that the "true" stable area, found numerically, is larger and in particular it contains the light area located between $f = 1$ and $f = 2$.

7. Conclusion. We have studied the trapped modes localized around an elastic plate placed in the center of a rigid waveguide and surrounded by a compressible fluid in a uniform flow. The case of real resonance frequencies was already known and we have extended the study to the search of complex frequencies corresponding to the development of instabilities. We have mainly proved two results: in the space (μ, U, c), there is a "stability" area in which no instability can develop. In particular it corresponds to $\mu < \mu_c$ or $U < U_c$ where μ_c and U_c are threshold values. Moreover, outside this stability area, if an instability of frequency ω develop, necessarily ω lies in a disc of bounded radius in the complex plane. A numerical study has confirmed these results.

A point that has not been discussed in the paper is the quality of the threshold estimates. In practice it appears that the theoretical threshold are rather far from the "real" thresholds found numerically, as shown in Fig. 7. For instance, instabilities are found numerically to develop for $U > U_c^{num}$ and the theoretical threshold U_c, obtained in closed form, is not a good approximation of U_c^{num} (see Fig. 6 (a) where $U_c = 0.18$ and $U_c^{num} = 0.4$). We do not know how to improve our estimates since we have already used Poincaré's inequalities with adjustable parameters (see Eq. (16) and (17)) to be the most accurate as we could. However, our results are useful since they define a stability area which, although it could be larger, gives a security area to avoid instabilities, which is what we wish the most in practice.

Appendix A. Modes of the duct.

A.1. Characterization of the modes. The acoustic propagation in the half duct without plate, in presence of a uniform flow, can be completely described by computing the modes of the duct. These modes are the solutions with separated

variables ($\varphi(x,y) = e^{i\beta x}\theta(y)$) of:

$$\left\{\begin{array}{rcl} \left(\dfrac{\partial^2}{\partial x^2} + \dfrac{1}{\alpha^2}\dfrac{\partial^2}{\partial y^2}\right)\varphi &=& \dfrac{1}{c^2}\left(U\dfrac{\partial}{\partial x} - i\omega\right)^2\varphi \quad \text{in} \quad \Omega, \\ \dfrac{\partial\varphi}{\partial y}(x,1) &=& 0 \quad \text{on} \quad \Sigma, \\ \varphi(x,0) &=& 0 \quad \text{for} \quad x \in \mathbb{R}. \end{array}\right.$$

Introducing the transverse functions

$$\theta_n(y) = \sqrt{2}\sin\left[\pi\left(n - \frac{1}{2}\right)y\right], n \geq 1,$$

forming a basis of $\{\theta(y) \in H^1(0,1)/\theta(0) = 0\}$, the modes read

$$\varphi_n^{\pm}(x,y) = e^{i\beta_n^{\pm}x}\theta_n(y),$$

with

$$\begin{aligned} \beta_n^{\pm} &= \frac{-kM \pm \gamma_n}{1-M^2} \quad \text{where} \quad k = \frac{\omega}{c}, \\ \gamma_n &= \sqrt{k^2 - (1-M^2)\zeta_n^2}, \\ \zeta_n &= \frac{\pi}{\alpha}\left(n - \frac{1}{2}\right), n \geq 1. \end{aligned} \tag{26}$$

To define γ_n, the chosen definition of the complex square root is: $\sqrt{z} = \sqrt{r}e^{i\theta/2}$ for $z = re^{i\theta}$, $\theta \in [0, 2\pi[$. This definition of the complex square root leads to $\Im m(\gamma_n) \geq 0$ for any $\omega \in \mathbb{C}$.

The characteristics of the modes depend on the nature of ω: $\omega \in \mathbb{R}$ or $\omega \in \mathbb{C}\backslash\mathbb{R}$.

• For real values of $\omega \in \mathbb{R}$, we get

$$\begin{aligned} \gamma_n &= \sqrt{k^2 - (1-M^2)\zeta_n^2} \quad \text{for} \quad n - \frac{1}{2} < \frac{k\alpha}{\pi\sqrt{1-M^2}}, \\ \gamma_n &= i\sqrt{(1-M^2)\zeta_n^2 - k^2} \quad \text{for} \quad n - \frac{1}{2} > \frac{k\alpha}{\pi\sqrt{1-M^2}}. \end{aligned}$$

Therefore a finite number of propagative modes ($\beta_n^{\pm} \in \mathbb{R}$) exist and an infinite number of evanescent modes ($\beta_n^{\pm} \in i\mathbb{R}$ with $\pm\Im m(\beta_n^{\pm}) > 0$) exist. The + modes "propagate" downstream: when they are propagative, they correspond to a positive group velocity and when they are evanescent, they decrease when $x \to \infty$. Symmetrically, the − modes propagate upstream.

For low frequencies, $k < k_c \equiv \pi\sqrt{1-M^2}/(2\alpha)$, the so-called cut-off wave number of the half-guide, all the modes are evanescent and this is a good framework when looking for trapped modes.

• For complex values of ω, $\omega \in \mathbb{C}\backslash\mathbb{R}$, all the modes are evanescent since it is straightforward to verify that $\pm\Im m(\beta_n^{\pm}) > 0$ and the + modes are downstream modes whereas the − modes are upstream modes.

A.2. Transparent boundary conditions. Let us point out that the duct modes are useful since every fluid vibration propagating outside the duct part including the plate can be decomposed on these modes. More precisely, if we introduce the vertical boundaries

$$\Sigma_R^{\pm} = \{(x,y), x = \pm R, y \in]0,1[\},$$

and remembering that the plate is of length 1, we have the

LEMMA 13. *For any $R > 1$, for any $\pm x \geq R$, a solution of (2) belonging to $H^1(\Omega)$ can be written:*

$$\varphi(x,y) = \sum_{n\geq 1} a_n^{\pm} e^{i\beta_n^{\pm}(x\mp R)}\theta_n(y), \tag{27}$$

with

$$a_n^{\pm} = (\varphi, \theta_n)_{\Sigma_R^{\pm}} \equiv \int_0^1 \varphi(\pm R, y)\theta_n(y)dy.$$

Proof. For any $x \notin [0,1]$, which corresponds to be located in the duct outside the plate, the velocity potential can be decomposed on the duct modes:

$$\varphi(x,y) = \sum_{n\geq 1} a_n^{\pm} e^{i\beta_n^{\pm}(x\mp R)}\theta_n(y).$$

The coefficient $a_n^{\pm}$ are deduced, using the orthogonality of the transverse functions

$$(\theta_n, \theta_m)_{\Sigma_R^{\pm}} = \delta_{mn} \text{ for any } n, m \geq 1.$$

□

Using (27), we can define (exact) transparent boundary conditions thanks to DtN (Dirichlet to Neumann) operators $T^{\pm}$: for any $R > 1$,

$$\begin{array}{rcl} \dfrac{\partial\varphi}{\partial x}(x=\pm R, y) & = & T^{\pm}\varphi(x=\pm R, y) \text{ with} \\ T^{\pm}: & & H^{1/2}(\Sigma_R^{\pm}) \to H^{-1/2}(\Sigma_R^{\pm}), \\ & & \varphi(\pm R, y) \to \pm i\beta_n^{\pm} \ (\varphi, \theta_n)_{\Sigma_R^{\pm}} \theta_n(y). \end{array} \tag{28}$$

Appendix B. Proof of lemma 3 for the continuous resonance problem.

To prove that if ω is a resonance frequency, then $\overline{\omega}$ is also a resonance frequency, we proceed in different steps:

- for the resonance problem (2) set in an unbounded domain, we define an equivalent formulation (29) set in a bounded domain,
- in the bounded domain, thanks to a compacity property we prove that the resonance problem is of Fredholm type,
- we conclude using the fact that $A^{\star}(\omega) = A(\overline{\omega})$ and the property $\operatorname{Ker} \mathrm{A}^{\star}(\omega) = (\operatorname{Ran} \mathrm{A}(\omega))^{\perp}$.

B.1. Resonance problem set in a bounded domain. Thanks to the definition of the radiation conditions at finite distance (28), we can introduce two equivalent ways to define the trapped modes: in an unbounded domain or in a domain bounded by radiation conditions. The unbounded problem has been defined in (2). The problem can also be set in a bounded domain, using the DtN operator (28) to write transparent boundary conditions on the boundaries of the domain. In this aim we note for any $R > 1$ (to include the whole plate)

$$\Omega_R = \{(x,y) \in \Omega, |x| < R\} \text{ and } \Gamma_R^{\pm} = \{(x,y) \in \Gamma^{\pm}, |x| < R\},$$

the bounded domains and we introduce the new solution space

$$V_R = \{\varphi \in H^1(\Omega_R), \varphi = 0 \text{ on } \Gamma_R^{\pm}\}.$$

Then the problem of finding trapped mode takes the form: Find $(\varphi, u) \in V_R \times W$ such that

$$
(29) \qquad \left\{ \begin{array}{rcl}
\left(\dfrac{\partial^2}{\partial x^2} + \dfrac{1}{\alpha^2}\dfrac{\partial^2}{\partial y^2}\right)\varphi & = & \dfrac{1}{c^2}\left(U\dfrac{\partial}{\partial x} - i\omega\right)^2 \varphi \quad \text{in} \quad \Omega_R, \\
\left(\dfrac{d^4}{dx^4} - \omega^2\right) u & = & 2\mu\left(U\dfrac{\partial}{\partial x} - i\omega\right)\varphi(x,0) \quad \text{on} \quad \Gamma, \\
\dfrac{1}{\alpha}\dfrac{\partial\varphi}{\partial y}(x,0) & = & \left(U\dfrac{\partial}{\partial x} - i\omega\right) u \quad \text{on} \quad \Gamma, \\
\dfrac{\partial\varphi}{\partial x} & = & \pm i\beta_n^{\pm}\ (\varphi,\theta_n)_{\Sigma_R^{\pm}}\,\theta_n(y) \quad \text{on} \quad \Sigma_R^{\pm}, \\
\dfrac{\partial\varphi}{\partial y}(x,1) & = & 0 \quad \text{on} \quad \Sigma_R, \\
u(0) = 0 = u'(0) & \text{and} & u''(1) = 0 = u^{(3)}(1).
\end{array} \right.
$$

To justify this problem we will prove that (29) is equivalent to (2).

B.2. Equivalence between the bounded and unbounded problems. Problems (2) and (29) are equivalent. One implication is easy: (2) implies (29) since (29) is obtained by restricting the solution of (2) to Ω_R. The reverse is less obvious but is true since a solution of (29) can be extended in a solution of (2), using (27). The only difficulty is to check that the extended solution is in $H^1(\Omega)$. When $\omega \in \mathbb{C}\backslash\mathbb{R}$, the fact that all the duct modes are evanescent insures that the extension belongs to $H^1(\Omega)$. When $\omega \in \mathbb{R}$, we have first to prove that the solution of (29) does not excite the propagating modes. In this aim, we write the variational form of (29):

(30) Find $(\varphi, u) \in V_R \times W$ such that $a_R[\omega; (\varphi, u), (\psi, v)] = 0$ for all $(\psi, v) \in V_R \times W$,

with

$$
a_R[\omega; (\varphi, u), (\psi, v)] = a_{fluid}[\omega; (\varphi, u), (\psi, v)] + a_{plate}[\omega; (\varphi, u), (\psi, v)],
$$

and

$$
a_{fluid}[\omega; (\varphi, u), (\psi, v)] =
$$

$$
\int_{\Omega_R} \left[(1 - M^2)\frac{\partial\varphi}{\partial x}\overline{\frac{\partial\psi}{\partial x}} + \frac{1}{\alpha^2}\frac{\partial\varphi}{\partial y}\overline{\frac{\partial\psi}{\partial y}} - i\frac{\omega}{c}M\left(\frac{\partial\varphi}{\partial x}\overline{\psi} - \varphi\overline{\frac{\partial\psi}{\partial x}}\right) - \frac{\omega^2}{c^2}\varphi\overline{\psi}\right],
$$

$$
+\frac{1}{\alpha}\int_{\Gamma}\overline{\psi}\left(U\frac{\partial u}{\partial x} - i\omega u\right) - i\sum_{n\geq 1}\gamma_n(\omega)\ (\varphi,\theta_n)_{\Sigma_R^{\pm}}\,(\theta_n,\psi)_{\Sigma_R^{\pm}},
$$

with γ_n defined in (26) and

$$
a_{plate}[\omega; (\varphi, u), (\psi, v)] = \frac{1}{2\mu\alpha}\int_{\Gamma}\left(\frac{d^2u}{dx^2}\frac{d^2\overline{v}}{dx^2} - \omega^2 u\overline{v}\right) + \frac{1}{\alpha}\int_{\Gamma}\varphi\left(U\frac{\partial\overline{v}}{\partial x} + i\omega\overline{v}\right).
$$

Then, choosing $(\psi, v) = (\varphi, u)$, we take the imaginary part of (30)

$$
\Im m\,(a_R[\omega; (\varphi, u), (\varphi, u)]) = 0, \quad \text{which leads to} \quad \sum_{n\geq 1}\Re e\,(\gamma_n)\ |\,(\varphi,\theta_n)_{\Sigma_R^{\pm}}\,|^2 = 0.
$$

Since $\Re e\,(\gamma_n) = 0$ for the evanecent modes for $\omega \in \mathbb{R}$, it leads to $(\varphi,\theta_n)_{\Sigma_R^{\pm}} = 0$ for all the propagating modes. Therefore the extended solution (27) is purely evanescent and belongs to $H^1(\Omega)$ and we have proved that (29) implies (2).

B.3. Fredholm alternative. Thanks to the Riesz theorem we can introduce the operator $A(\omega)$ such that for all (φ, u) in $V_R \times W$ and all (ψ, v) in $V_R \times W$,

$$(A(\omega)(\varphi, u), (\psi, v))_{V_R \times W} = a_R[\omega; (\varphi, u), (\psi, v)],$$

where we use the scalar product on $V_R \times W$:

$$((\varphi, u), (\psi, v))_{V_R \times W} =$$

$$\int_{\Omega_R} \left[\frac{\partial \varphi}{\partial x} \overline{\frac{\partial \psi}{\partial x}} + \frac{\partial \varphi}{\partial y} \overline{\frac{\partial \psi}{\partial y}} + \varphi \overline{\psi} \right] dxdy + \int_\Gamma \left(\frac{d^2 u}{dx^2} \frac{d^2 \overline{v}}{dx^2} + \frac{du}{dx} \frac{d\overline{v}}{dx} + u\overline{v} \right) dx.$$

Then the problem (30) can be written in an operator form: find $\omega \in \mathbb{C}$ such that exists (φ, u) in $V_R \times W$ satisfying $A(\omega)(\varphi, u) = 0$. The operator A is decomposed as $A = B + C$ where

- $$(B(\omega)(\varphi, u), (\psi, v))_{V_R \times W} = \int_{\Omega_R} \left[(1 - M^2) \frac{\partial \varphi}{\partial x} \overline{\frac{\partial \psi}{\partial x}} + \frac{1}{\alpha^2} \frac{\partial \varphi}{\partial y} \overline{\frac{\partial \psi}{\partial y}} + \varphi \overline{\psi} \right],$$

$$\frac{1}{2\mu\alpha} \int_\Gamma \left(\frac{d^2 u}{dx^2} \frac{d^2 \overline{v}}{dx^2} + u\overline{v} \right) - i \sum_{n \geq 1} \gamma_n(\omega) \ (\varphi, \theta_n)_{\Sigma_R^\pm} (\theta_n, \psi)_{\Sigma_R^\pm},$$

- $$(C(\omega)(\varphi, u), (\psi, v))_{V_R \times W} = \int_{\Omega_R} \left[-i \frac{\omega}{c} M \left(\frac{\partial \varphi}{\partial x} \overline{\psi} - \varphi \overline{\frac{\partial \psi}{\partial x}} \right) - \left(1 + \frac{\omega^2}{c^2} \right) \varphi \overline{\psi} \right],$$

$$+ \frac{1}{\alpha} \int_\Gamma \overline{\psi} \left(U \frac{\partial u}{\partial x} - i\omega u \right) - \frac{1 + \omega^2}{2\mu\alpha} \int_\Gamma u\overline{v} + \frac{1}{\alpha} \int_\Gamma \varphi \left(U \frac{\partial \overline{v}}{\partial x} + i\omega \overline{v} \right).$$

The sesquilinear form $b_R[\omega; (\varphi, u), (\psi, v)] = (B(\omega)(\varphi, u), (\psi, v))_{V_R \times W}$ is coercive on $V_R \times W$ which proves that $B(\omega)$ is an isomorphism of $V_R \times W$. Indeed

$$\exists C_R > 0, \forall (\varphi, u) \in V_R \times W, \Re e \left(b_R[\omega; (\varphi, u), (\varphi, u)] \right) \geq C_R ||(\varphi, u)||^2_{V_R \times W}.$$

The key point is that

$$\Re e \left(-i \sum_{n \geq 1} \gamma_n(\omega) \ (\varphi, \theta_n)_{\Sigma_R^\pm} (\theta_n, \varphi)_{\Sigma_R^\pm} \right) = \sum_{n \geq 1} \Im m \left(\gamma_n \right) \ | (\varphi, \theta_n)_{\Sigma_R^\pm} |^2 \geq 0,$$

since $\Im m(\gamma_n(\omega)) \geq 0$. It is also straightforward to prove that $C(\omega)$ is a compact operator on $V_R \times W$, the key point being the Rellich theorem which applies since Ω_R is bounded.

The resonance problem $(B + C)(\varphi, u) = 0$ can be written $(I + B^{-1}C)(\varphi, u) = 0$ because B is an isomorphism. And finally since $B^{-1}C$ is a compact operator, the Fredholm alternative holds for this equation.

B.4. Characteristics of the eignevalues. The Fredholm property obtained in the previous paragraph implies in particular, for the operator $S = I + B^{-1}C$ but also for the operator $A \equiv BS = B + C$ (since B is an isomorphism), that

- $\mathrm{Ker\,A}(\omega) = \{0\} \Leftrightarrow \mathrm{Ran\,A}(\omega) = \mathrm{V_R \times W}$,
- $\mathrm{Ker\,A}^\star(\omega) = (\mathrm{Ran\,A}(\omega))^\perp$ where $A^\star(\omega)$ is the adjoint of $A(\omega)$.

Moreover it is easy to prove $A^\star(\omega) = A(\overline{\omega})$. This is in particular due to $\gamma_n(\overline{\omega}) = -\overline{\gamma_n(\omega)}$.

Therefore, combining together the previous results, we get $\operatorname{Ker} \mathrm{A}(\omega) = \{0\} \Leftrightarrow \operatorname{Ran} \mathrm{A}(\omega) = \mathrm{V_R} \times \mathrm{W} \Leftrightarrow \operatorname{Ker} \mathrm{A}^\star(\omega) = \{0\}$. In other words $\operatorname{Ker} \mathrm{A}(\omega) \neq \{0\} \Leftrightarrow \operatorname{Ker} \mathrm{A}(\overline{\omega}) \neq \{0\}$ and thus if ω is a resonance frequency, then $\overline{\omega}$ is also a resonance frequency.

Finally, we have proved that if ω is an eigenvalue then $\pm\overline{\omega}$ are also eigenvalues. But then, since $\overline{\omega}$ is an eigenvalue, $\pm\omega$ are also eigenvalues which ends the proof of lemma 3.

Appendix C. Numerical method.

We start from the formulation of the trapped modes problem set in a bounded domain (30). Noting $(w_j)_{j=1\cdots N_{\mathrm{dof}}}$ the finite element basis (P1 elements) with N_{dof} the number of degrees of freedom, the velocity potential is sought under the form

$$\varphi = \sum_{j=1}^{N_{\mathrm{dof}}} \varphi_j w_j(x,y),$$

where the nodal values φ_j are unknowns. Also using the modal basis of the plate $(\xi_m)_{m\geq 1}$ Eq. (33), the displacement of the plate is sought under the form

$$u = \sum_{n=1}^{N_{\mathrm{pl}}} u_n \xi_n(x),$$

where the modal components u_n are unknowns and N_{pl} is the number of plate modes taken into account. Then, developing

$$a_{fluid}\left[\omega; \left(\sum_{j=1}^{N_{\mathrm{dof}}} \varphi_j w_j, \sum_{n=1}^{N_{\mathrm{pl}}} u_n \xi_n\right), (w_i, \xi_m)\right] = 0,$$

and

$$a_{plate}\left[\omega; \left(\sum_{j=1}^{N_{\mathrm{dof}}} \varphi_j w_j, \sum_{j=1}^{N_{\mathrm{pl}}} u_n \xi_n\right), (w_i, \xi_m)\right] = 0,$$

for all $i = 1$ to N_{dof} and all $m = 1$ to N_{pl}, we are lead to define the matrices

$$D_{ij} = (1-M^2)\left(\frac{\partial w_j}{\partial x}, \frac{\partial w_i}{\partial x}\right)_{\Omega_R} + \frac{1}{\alpha^2}\left(\frac{\partial w_j}{\partial y}, \frac{\partial w_i}{\partial y}\right)_{\Omega_R},$$

$$E_{ij} = \frac{M}{c}\left[\left(w_j, \frac{\partial w_i}{\partial x}\right)_{\Omega_R} - \left(\frac{\partial w_j}{\partial x}, w_i\right)_{\Omega_R}\right],$$

$$M_{ij}(\omega) = -i\sum_{p=1}^{N_{\mathrm{DtN}}} \gamma_p(\omega)\zeta_p \left(w_j, \theta_p\right)_{\Sigma_R^\pm} \left(\theta_p, w_i\right)_{\Sigma_R^\pm},$$

and

$$F_{ij} = \left(-\frac{1}{c^2}\right)(w_j, w_i)_{\Omega_R}, \quad G_{in} = \frac{U}{\alpha}\left(\frac{d\xi_n}{dx}, w_i\right)_\Gamma, \quad H_{in} = \left(-\frac{1}{\alpha}\right)(\xi_n, w_i)_\Gamma,$$

$$I_{mn} = \frac{1}{2\mu\alpha}\left(\frac{d^2\xi_n}{dx^2}, \frac{d^2\xi_m}{dx^2}\right)_\Gamma, \quad J_{mn} = \left(-\frac{1}{2\mu\alpha}\right)(\xi_n, \xi_m)_\Gamma.$$

N_{DtN} is the number of term taken to describe the DtN operators. Thanks to the defined matrices, the discretized resonance problem is

$$\begin{pmatrix} D + i\omega E + \omega^2 F + M(\omega) & G + i\omega H \\ G^T - i\omega H^T & I + \omega^2 J \end{pmatrix} \begin{pmatrix} \Phi \\ U \end{pmatrix} = 0, \tag{31}$$

where we have introduced the vectors of unknowns

$$\Phi = (\varphi_1, \cdots, \varphi_{N_{\mathrm{dof}}})^T \ \text{ and } \ U = \left(\xi_1, \cdots, \xi_{N_{\mathrm{pl}}}\right)^T.$$

This is a non-linear eigenvalue problem because of the matrix $M(\omega)$ which includes $\gamma_n(\omega)$ defined in Eq. (26) as a square root of ω. To simplify the study, we have approximated the matrix M to get a quadratic eigenvalues problem. Several approaches are possible and we have checked that they give very similar results. The simplest possibility is to replace the transparent boundary conditions (28) by homogeneous Neumann or Dirichlet boundary conditions:

$$\frac{\partial \varphi}{\partial x} = 0 \ \text{ or } \ \varphi = 0 \ \text{ on } \ \Sigma_R^{\pm}.$$

Since the velocity potential decreases exponentially away from the plate, these approximations are very good if $\Sigma_R^{\pm}$ is far enough from the plate. In both cases, we get that the matrix $M = 0$. The Dirichlet case requires an extra element: the finite element basis $(w_j)_{j=1\cdots N_{\mathrm{dof}}}$ must satisfy the Dirichlet condition.

We have chosen another approach which consists in replacing $\gamma_n = \sqrt{k^2 - (1-M^2)\zeta_n^2}$ by the approximation $\tilde{\gamma}_n = i\sqrt{1-M^2}\zeta_n$. This is the natural approximation when $n \to \infty$. It leads to the approximation $\tilde{M}$ of the matrix M, independent of the frequency and defined by

$$\tilde{M}_{ij} = \sqrt{1-M^2} \sum_{p=1}^{N_{\mathrm{DtN}}} \zeta_p \left(w_j, \theta_p\right)_{\Sigma_R^{\pm}} \left(\theta_p, w_i\right)_{\Sigma_R^{\pm}}.$$

We have chosen this approximation because it is close from the true radiation conditions and it becomes exact for large p values. Moreover it is easy to implement numerically.

To write the quadratic eigenvalue problem as a classical eigenvalue problem, we introduce the matrices:

$$A = \begin{pmatrix} D + M & G \\ G^T & 0 \end{pmatrix}, \ B = \begin{pmatrix} E & H \\ -H^T & 0 \end{pmatrix}, \ C = \begin{pmatrix} F & 0 \\ 0 & J \end{pmatrix},$$

where A, B and C are real matrices with $A^T = A$, $B^T = -B$ (since $E^T = -E$) and $C^T = C$. Then (31) reads

$$(A + i\omega B + \omega^2 C)X = 0,$$

where X is the vector $(\Phi, U)^T$.

The Finite Element matrices are built using a Finite Elements code [33] and the eigenvalues are determined using the Matlab software. For a domain of size 2×1, we use an unstructured triangular mesh, we introduce P1 finite elements and in practice we take $N_{\mathrm{dof}} = 2309$, $N_{\mathrm{pl}} = 6$ and $N_{\mathrm{DtN}} = 10$. We have checked that taking larger values doesn't change significantly the results.

Appendix D. Simplification of the theoretical estimates.

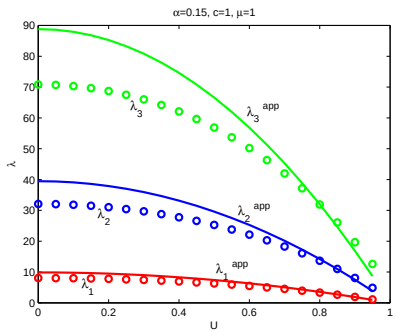

FIG. 8. *Three first eigenvalues λ_n of problem (32) versus U for $\alpha = 0.15$ and $c = 1$. Circles: exact values, Solid lines: approximations λ_n^{app}*

Here we show that $\hat{\sigma}$ defined in (11) can be approximated by (20) that we recall

$$\sigma = \min\left[(c^2 - U^2)\pi^2, \alpha_1^4\right].$$

Indeed the values of λ_1 and α_1^4, introduced in (8) and (10), can be obtained in closed form, as explained now.

• Approximation of λ_1:

Since

$$\lambda_1 = \inf_{\varphi \in V} R(\varphi),$$

with R defined in (9), using the test field $\varphi_0 \in V$ defined by

$$\left\{ \begin{array}{lcll} \varphi_0(x,y) & = & \sin(\pi x) & \text{for} \quad x \in]0,1[, \\ \varphi_0(x,y) & = & 0 & \text{for} \quad x \notin]0,1[, \end{array} \right.$$

we find the upper bound

$$\lambda_1 \leq R(\varphi_0) = (c^2 - U^2)\pi^2.$$

We have determined numerically that this upper bound $(c^2 - U^2)\pi^2$ is in fact a good approximation of λ_1. To do so and to find the numerical value of λ_1, we notice that λ_1 is also the first eigenvalues of the problem: find $\varphi \in V$ and $\lambda \in \mathbb{R}$ such that

$$\left\{ \begin{array}{l} -(c^2 - U^2)\dfrac{\partial^2 \varphi}{\partial x^2} - \dfrac{c^2}{\alpha^2}\dfrac{\partial^2 \varphi}{\partial y^2} = \lambda \varphi \quad \text{in} \quad \Omega, \\ \dfrac{1}{\alpha}\dfrac{\partial \varphi}{\partial y}(x,0) = 0 \quad \text{on} \quad \Gamma, \\ \dfrac{\partial \varphi}{\partial y}(x,1) = 0 \quad \text{on} \quad \Sigma. \end{array} \right. \tag{32}$$

Indeed the Min-Max principle indicates that λ_1 defined by (8) thanks to the Rayleigh quotient (9) is the first eigenvalue if $\lambda_1 < (\pi c/2\alpha)^2$ (below the essential spectrum).

For $\alpha = 0.15$ and $c = 1$, in Fig. 8 are plotted with solid lines the three first eigenvalues λ_n, $n = 1$, 2 and 3, of problem (32) versus U below the essential spectrum ($(\pi c/2\alpha)^2 \simeq 110$), obtained numerically thanks to a Finite Element method. The circles represent the values $\lambda_n^{\text{app}} \equiv n^2\pi^2(c^2 - U^2)$ versus U for $n = 1$, 2 and 3. We see that for $n = 1$, $\lambda_1^{\text{app}} = \pi^2(c^2 - U^2)$ approximates very accurately λ_1. On the

contrary, the approximations λ_n^{app} of λ_n for $n = 2$ and 3 are not satisfactory (they become better approximations when α is decreased, result not reported here).

• Approximation of α_1:

To determine α_1, we introduce the following eigenvalue problem: find $u \in W$ and $\lambda^{\text{plate}} \in \mathbb{R}$ such that

$$\frac{d^4u}{dx^4} = \lambda^{\text{plate}} u \quad \text{for} \quad x \in]0,1[,$$
$$u''(1) = 0 = u^{(3)}(1).$$

This is the equation of the plate in vacuum and the eigenvalues λ_n^{plate} are equal to the square of the eigenfrequencies ω_n^{plate} of the plate. A simple explicit calculation shows that $\lambda_n^{\text{plate}} = \alpha_n^4$ with α_n satisfying [1, 9]

$$\cos\alpha_n \cosh\alpha_n = -1.$$

In particular, $\alpha_1 = 1.88$. The eigenmodes are

$$\xi_n(x) = A_n\left[\sinh(\alpha_n x) - \sin(\alpha_n x)\right] + B_n\left[\cosh(\alpha_n x) - \cos(\alpha_n x)\right], \tag{33}$$

where

$$B_n = -A_n \frac{\sinh(\alpha_n) + \sin(\alpha_n)}{\cosh(\alpha_n) + \cos(\alpha_n)},$$

and A_n can be chosen such that $\displaystyle\int_\Gamma |\xi_n|^2 = 1$. Finally the Min-Max principle indicates that λ_1^{plate} satisfies

$$\lambda_1^{\text{plate}} = \inf_{u \in W} \frac{\int_\Gamma \left|\frac{d^2u}{dx^2}\right|^2}{\int_\Gamma |u|^2},$$

in accordance with (10).

REFERENCES

[1] A.-S. Bonnet-Ben Dhia, and J.-F. Mercier, "Resonances of an elastic plate in a compressible confined fluid.", The Quarterly Journal of Mechanics and Applied Mathematics 60(4), 397-421 (2007)

[2] A.-S. Bonnet-Ben Dhia, and J.-F. Mercier, "Resonances of an elastic plate coupled with a compressible confined flow.", The Quarterly Journal of Mechanics and Applied Mathematics 62(2), 105-129 (2009)

[3] H. Dowell, C. Curtiss Jr., R. H. Scanlan, F. Sisto, "A Modern Course in Aeroelasticity", Kluwer Academic Publishers (1989)

[4] Y.C. Fung, "An Introduction to the Theory of Aeroelasticity", J. Wiley, New York (1955)

[5] C. Eloy, R. Lagrange, C. Souilliez and L. Schouveiler, "Aeroelastic instability of cantilevered flexible plates in uniform flow", J. Fluid Mech. 611, 97106 (2008)

[6] Y. Watanabe, S. Suzuki, M. Sugihara and Y. Sueoka, "An Experimental Study of Paper Flutter", Journal of Fluids and Structures 16(4), 529542 (2002)

[7] Y. Watanabe, K. Isogai and S. Suzuki and M. Sugihara, "A Theoretical Study of Paper Flutter", Journal of Fluids and Structures 16(4) 543560 (2002)

[8] T. S. Balint and A. D. Lucey, "Instability of a cantilevered flexible plate in viscous channel flow", Journal of Fluids and Structures 20, 893912 (2005)

[9] C. Q. Guo and M. P. Paidoussis, "Stability of rectangular plates with free side-edges in two-dimensional inviscid channel flow.", Journal of Applied Mechanics 67(1) 171-176 (2000)

[10] D. V. Evans, M. Levitin, and D. Vassiliev, "Existence theorems for trapped modes.", Journal of Fluid Mechanics 261, 21-31 (1994)

[11] E. B. Davies, and L. Parnovski, "Trapped modes in acoustic waveguides.", The Quarterly Journal of Mechanics and Applied Mathematics 51(3), 477-492 (1998)
[12] N. S. A. Khallaf, L. Parnovski, and D. Vassiliev, "Trapped modes in a waveguide with a long obstacle.", Journal of Fluid Mechanics 403, 251-261 (2000)
[13] E. J. Brambley, and N. Peake, "Stability and acoustic scattering in a cylindrical thin shell containing compressible mean flow.", Journal of Fluid Mechanics 602, 403-426 (2008)
[14] M. Vullierme-Ledard, "Asymptotic study of the vibration problem for an elastic body deeply immersed in an incompressible fluid", Math. Model. Numer. Anal. 19, 145-170 (1985)
[15] E. Sanchez-Palencia, "Nonhomogeneous media and vibration theory", Springer-Verlag, Berlin (1980)
[16] R. Ohayon and E. Sanchez-Palencia, "On the vibration problem for an elastic body surrounded by a slightly compressible fluid", RAIRO Anal. Numr. 17, 311-326 (1983)
[17] J. Sanchez-Hubert and E. Sanchez-Palencia, "Vibration and Coupling of Continuous Systems, Asymptotics Methods", Springer-Verlag, Berlin (1989)
[18] C. Conca, A. Osses, and J. Planchard, "Asymptotic Analysis Relating Spectral Models in Fluid–Solid Vibrations", SIAM journal on numerical analysis 35(3), 1020-1048 (1998)
[19] P. Destuynder and E. Gout-D'hénin, "Existence and uniqueness of a solution to an aeroacoustic model", Chinese Ann. Math. Ser. B 23, 11-24 (2002)
[20] P. Destuynder and J. Vétillard, "Modelling and control of noise in a flexible flow duct.", Computer Methods in Applied Mechanics and Engineering 197(19), 1801-1812 (2008)
[21] L. Cot, J-P. Raymond, and J. Vancostenoble, "Exact controllability of an aeroacoustic model with a Neumann and a Dirichlet boundary control", SIAM Journal on Control and Optimization 48(3), 1489-1518 (2009)
[22] J. Vétillard and P. Destuynder, "A noise control problem arising in a flow duct", SIAM Journal on Applied Mathematics 64(6), 1987-2017 (2004)
[23] D. V. Evans, C. M. Linton, and F. Ursell, "Trapped mode frequencies embedded in the continuous spectrum.", The Quarterly Journal of Mechanics and Applied Mathematics 46(2), 253-274 (1993):
[24] M. D. Groves, "Examples of Embedded Eigenvalues for Problems in Acoustic Waveguides", Mathematical Methods in the Applied Sciences 21(6), 479-488 (1998)
[25] Porter, R., and D. V. Evans, "Embedded RayleighBloch surface waves along periodic rectangular arrays.", Wave motion 43(1), 29-50 (2005)
[26] L. J. Ayton, J. R. Gill and N. Peake, "The importance of the unsteady Kutta condition when modelling gustaerofoil interaction.", Journal of Sound and Vibration, 378, 28-37 (2016).
[27] W. Koch, "Resonant Acoustic Frequencies of Flat Plate Cascades", Journal of Sound and Vibration 88(2), 233-242 (1983)
[28] N.C. Ovenden, W. Eversman, S.W. Rienstra, "Cut-on cut-off transition in flow ducts: comparing multiple-scales and finite-element solutions", Paper AIAA 2004-2945 of the 10th AIAA/CEAS Aeroacoustics Conference, Manchester, UK, 10-12 May 2004
[29] A. Aslanyan, L. Parnovski, and D. Vassiliev, "Complex resonances in acoustic waveguides.", The Quarterly Journal of Mechanics and Applied Mathematics 53(3), 429-447 (2000)
[30] Y. Duan, et al., "Complex resonances and trapped modes in ducted domains." Journal of Fluid Mechanics 571, 119-147 (2007)
[31] M. Lenoir, M. Vullierme-Ledard, and C. Hazard, "Variational formulations for the determination of resonant states in scattering problems.", SIAM journal on mathematical analysis 23(3), 579-608 (1992)
[32] C. Hazard, and M. Lenoir, "Determination of scattering frequencies for an elastic floating body.", SIAM journal on mathematical analysis 24(6), 1458-1514 (1993)
[33] XLiFE++, eXtended Library of Finite Elements in C++, https://uma.ensta-paristech.fr/soft/XLiFE++/